OMAE2014-24089

MODEL SCALE ANALYSIS OF A TLP FLOATING OFFSHORE WIND TURBINE

Ricardo Zamora-Rodriguez

Model Basin Res. Gr. (CEHINAV), Naval Architecture Department (ETSIN), Technical University of Madrid (UPM), Madrid, Spain. Email: ricardo.zamora@upm.es

Juan Amate-Lopez

IBERDROLA INGENIERIA, Madrid, Spain. Email: jaez@iberdrola.es

Pasquale Dinoi

Model Basin Res. Gr. (CEHINAV), Naval Architecture Department (ETSIN), Technical University of Madrid (UPM), Madrid, Spain.

Pablo Gomez-Alonso

IBERDROLA INGENIERIA, Madrid, Spain. Email: pgns@iberdrola.es

Victor De-Diego-Martin

IBERDROLA INGENIERIA, Madrid, Spain. Email: vdma@iberdrola.es

Alexandre N. Simos

Numerical Offshore Tank (TPN), University of São Paulo, São Paulo, Brazil Email: alesimos@usp.br

Antonio Souto-Iglesias

Model Basin Res. Gr. (CEHINAV), Naval Architecture Department (ETSIN), Technical University of Madrid (UPM), Madrid, Spain.

ABSTRACT

This paper discusses the experimental campaign conducted by CEHINAV-UPM research group as request of IBERDROLA within the OCEAN LIDER RD project framework. The purpose of the campaign has been the hydrodynamic performance of a tension leg platform to support a wind energy turbine (TLPWT). The turbine chosen in this study has been the 5MW reference WT of NREL, the location depth has been 80m and the operation area is Estaca de Bares in the north-west of Spain. Regular waves, operational, survival, failure and transport experiments have been

conducted. All tests have been performed in CEHINAV (UPM) model basin, except survival tests performed in CEHIPAR ocean basin. This document presents the experimental setup and results from decay tests, regular wave motion RAOs, irregular wave responses, tendon loads and accelerations. Experimental results are compared with available in-house numerical simulations and other numerical and experimental results found in literature.

MOTIVATION

In recent years, some of the most prominent Spanish electrical companies have undertaken research projects aimed at producing electricity with Floating Offshore Wind Turbines (FOWTs). The tension leg platform wind turbine (TLPWT) concept has been the one chosen by IBERDROLA for this initiative.

The TLP concept has the benefit of providing highly stiff restraint to heave, pitch and roll motions, with typical values one order of magnitude smaller those for a spar or a semi-submersible design of similar dimensions. The natural periods of a TLPWT are very short for the vertical plane motions (heave, roll and pitch) and quite long for horizontal plane motions (surge and sway in particular). This allows to design the TLP outside first order wave excitations for these motions, while symmetry and pontoons vertical position guarantees low yaw excitations. The main challenge for TLPWT resides in making the mooring system and installation cost-competitive [1].

The floating turbine response is rather complex and reflects the wind turbine aerodynamics, tower elastic modes, wind turbine controls, incident waves, floating platform dynamics and the mooring dynamics of the floating platform.

Crozier [2] did an extensive numerical analysis of two TLPWT designs, one to be towed to operation destination and another to be transported. She found that the transported TLPWT was the most cost competitive design whereas the towed TLP presented a more favorable dynamic performance. She used a 4 pontoons platform each with two tendons to which present design is similar.

Bachynski & Moan [3,4] presented the results of numerical modeling of an array of conceptual TLP FOWT designs. The dynamic response in different wave and wind conditions and using three different hydrodynamic models was analyzed. Results indicate that second order wave forces have a small effects on the structural load predictions. The tendon tension increased around 2-10 % in extremal sea condition, while neglible effects were observed in operational conditions. A set of TLPWT designs with a range of displacement of 846-12187 tons, with stiffness provided by 3 to 8 tendons, and waterline diameter 4.5-18 m, were analyzed. The documented models present these features [4]:

- 1. Surge natural period: 25 to 60 s
- 2. Heave natural period: 1-2.3 s
- 3. The coupled platform pitch and tower bending mode is typically found 3.5-4.5 s.

Bae & Kim [5] analyzed second order effects. A monocolumn TLP with 5 MW turbine and 4 spokes, in 200m water depth was considered. They found that second order sumfrequency wave loading introduces high frequency excitations near pitch/roll resonance frequencies or lowest tower flexural mode. Its effect is more clearly seen in the uncoupled case due to the lack of aerodynamic damping. Their method integrates ro-

tor dynamics and control, aero-dynamics, tower elasticity, floater dynamics, and mooring-line dynamics in time-domain.

Jagdale&Ma [6] analyzed a four pontoons TLP design using a time domain solver. They parametrically changed certain characteristics (tower length, pontoon length and cross-section and number of mooring lines) assessing the effect of such changes in the dynamic response of the platform.

Nihei et al. [7] built a TLPWT model trying to reproduce the elastic properties of the structure. Tests were conducted measuring the bending moment at the base of the tower and the tensions at the tendons. They did not find any slack event even in heavy seas. It is not clear how the operation depth was scaled in the experiments.

Nihei et al. [8] proposed a light design with three spokes and 6 tendons. They found in experiments that slack occurred on tendons and subsequent capsizing of the structure, which they were able to relate to drift mechanisms. They produced alternative designs and found experimentally no capsizing for them. Their scale was 1:100, substantially larger than the present research.

Naqvi et al 2012 [9] consider a TLPWT with scale 1:100 and 5MW turbine, shows that surge motion of the platform is dominating respect to other motion and varying tether pretension has little effect on response amplitude operator values.

Thiagarajan et al. [10] presented a theoretical framework for pitch motions based on simplified model of the thrust coefficient of the turbine blades.

Koo et al. [11] analyzed a three pontoons TLP platform design with time domain solver MLTSIM-FAST. They were able to reasonably reproduce operational response and tendon spectra. They used as validation reference the experimental works [12,13] which in turn followed the methodology from Martin et al. [14] FOWT testing of model scale.

The present work design has some particularities the authors believe could make this article relevant for the hydrodynamic community. First, a relatively low depth location has been selected, and second available experimental data in the literature for the type and number of pontoons and tendons is scarce. These two features made the numerical modeling difficult. With the aim of investigating such factors and to help in validating the numerical models, IBERDROLA set up the present experimental research campaign, which this paper documents.

The paper is organized as follows: first, platform main dimensions are summarized, following with main characteristics of model scale and experimental setup. Following, decay tests results, regular waves motion and tension RAOs, irregular survival results and towing experiments results are presented. and compared when possible with literature. Finally, some conclusions are drawn and future research prospects are suggested.

CASE STUDY AND EXPERIMENTAL SETUP

The Iberdrola TLPWT platform consists of a central cylindrical column with four square section pontoons (perpendicularly symmetrically distributed) attached at its bottom, each with two tendons (Fig. 1), aimed at supporting a 5MW generator, positioned at a height of 89m from MSL. The tendons are made of steel with 6x37 wires.

Each of the outer ends of the four pontoons incorporates two porches which allow the connection of the two tauted mooring lines per pontoon characteristics of this particular design. These two lines per pontoon assure a complete redundancy of the mooring system and guarantee stability in operational and survival conditions even in case of break of one line (the TLP can operate and survive only with one of these tauted lines). Mooring lines can be fabricated of steel or synthetic material depending on the specific conditions of the site and available supply chain.

The lower ends of the mooring lines will be connected to suction pile foundations (driven or drilled piles could be also an option depending on specific soil conditions). The optimal solution will be selected depending on soil type and market conditions. In most of soil types suction piles are accepted and it is a solution that barely impacts into the environment in comparison to another proposed solutions. Also "cluster suction piles" allows the installation of the two mooring lines rapidly and accurately to ease the full mooring lines installation operations.

The Iberdrola TLP can be built in standard dry-docks. The Wind Turbine will be pre-assembled on-shore previous to the launching operation (top left panel of Fig. 6). Four floaters will be attached to the end of the pontoons by means of a "gripper system", allowing increasing the stability of the system for the transportation and installation operations (top center panel of Fig. 6). A regular tug-vessel will be used in order to tow the complete system to the site (top right panel of Fig. 6). TLP tendons and suction cluster piles can be pre-installed in a different operation, before performing the main installation operation of the TLP+WT. The installed tether lines will account some subsea floaters to keep them erected, as well as some surface marking buoys to give a good location reference to the TLP installation spread (bottom left panel of Fig. 6). Once the TLP+WT device is over the marked location, a specifically designed ballast system will start the operation of lowering down the TLP until its final operational draught, when the connection to the tendons will be done (bottom center panel of Fig. 6). Once the tendon lines have been loaded (gently de-ballasting), floaters can be easily removed for its utilization in the installation of another TLP (bottom right panel of Fig. 6). This procedure allows fully transportation and installation of the wind turbine with standard type-boats and reduced weather windows. Model tests of transportation operations have been also carried out at the CEHINAV-UPM model basin, and will be further discussed in upcoming publications.

A reduced scale (1:40) model of the platform has been built from aluminum. The scale factor has been defined in order to

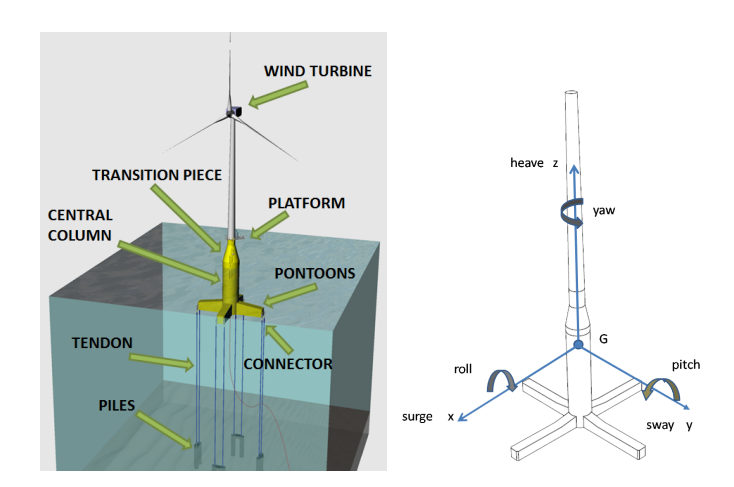


FIGURE 1. Floating wind turbine case study (left). System of reference (right)

properly scale the platform depth operation, considering CEHI-NAV model basin depth. Fig. 7 shows two pictures taken during the experiments in the CEHINAV Model Basin and in the CEHIPAR Ocean Basin (where survival tests were conducted). The main features of the platform, with the corresponding scaled values, are displayed in Table 1. The system of reference is presented in Fig. 1 with the origin in the the center of gravity.

	Prototype Scale	Model Scale
Lightship Weight	1050 [t]	16 [kg]
Displacement [MSL]	4333.7 [t]	66.06 [kg]
Draft	39.8 [m]	1.00 [m]
Pontoon Length	27.7 [m]	0.69 [m]
Freeboard	17.0 [m]	0.42 [m]
Number of Lines	8	8
Water Depth	80 [m]	2 [m]

TABLE 1. Main features of the model

The mooring lines have been manufactured with aluminum wire. Tendon rigidity is simulated using calibrated springs situated at the lower end of the tether lines. In Fig. 2 the mooring connections between tank bottom and the platform are shown.

Two accelerometers have been placed at CoG and nacelle. Motions have been measured with an optical tracking system (OPTITRACK). Line tensions have been measured with eight waterproof force transducers placed at the base of the tendons (left panel of Fig. 2). In order to take into account the wind ef-

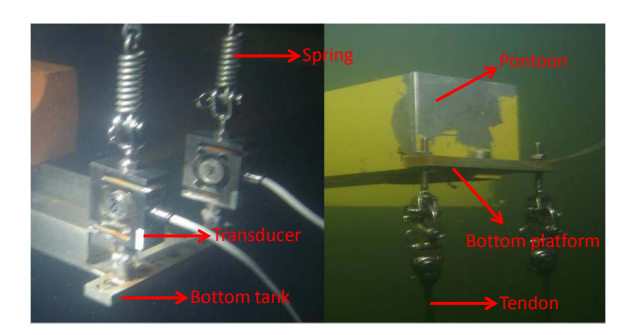


FIGURE 2. Mooring line connection with tank bottom (left) and with pontoons (right)

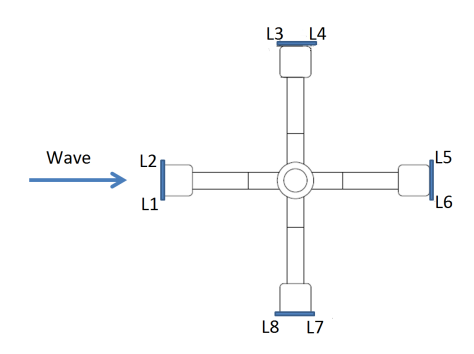


FIGURE 3. Plan view of platform showing the number of lines

fect a turbine has been positioned at the top of the tower. The turbine produces thrust action only in the *x* direction. The turbine thrust depends on the relative wind speed, which in turn, is mainly function of surge and sway velocities. Motion information is transferred in real time from OPTITRACK system to the turbine control in order to adjust the thrust accordingly.

Two environmental conditions are presented in this paper corresponding to *operational* (OC) and *survival* (SC) conditions with the characteristic values reported in Tab. 2. Operational conditions were selected following DNV standards [15] with respect to metocean data from "Estaca de Bares" buoy. The survival condition corresponds to 50 years return period storm conditions [15]. For this survival condition, rotor is parked to avoid damaging the wind turbine. In both conditions the turbine thrust and wind drag are simulated using FAST and conveniently scaled down.

In the following, all results are presented at prototype scale.

RESULTS: DECAY TESTS

The objective of the decay tests is to determine the damping coefficient and the natural periods in every degree of freedom. The focus will be on decay test results for horizontal plane motions (surge, sway and yaw). Decay test in vertical plane (heave,

	H_s	T_p	WS	WT
	(m)	(s)	(m/s)	
OC	2.5	10	11.4	NTM
SC	14.5	15.2	50	EWM

TABLE 2. Metocean conditions. Operational (OC). Survival (SC). Wind speed (WS). IEC Wind Type (WT). Normal turbulence model (NTM). Extreme Wind Model (EWM)

Motion	T[s]
Surge-Sway	25.21
Heave	1.09
Roll-Pitch	3.88
Yaw	11.42

TABLE 3. Natural Periods TLPWT

roll and pitch) measurements are harder due to system having a very large stiffness for those motions. Only natural periods will be provided for the latter.

Natural periods are presented in Table 3. It can be observed that all periods except yaw fall outside first order wave excitation. In regards to yaw, due to the platform symmetry and considering the pontoons position, far from the free surface, excitation is small, with damping taking a standard value ($\sim 8\%$). Under these conditions, yaw motions have remained, even when subjected to large excitation, very small.

The periods are similar to the ones reported for a 3 pontoons TLPWT, in computations with BLADED by Henderson et al. [1], and in model tests by Koo et al. [13]. A surge natural period significantly larger is shown by the latter ($\sim 39s$). However, their water depth is 200m compared to 80m in present design, with this difference being partially responsible for the shift in surge natural period. In regards to surge (or sway) motion, some selected samples of decay test repetitions are presented in Fig. 4. Experimental curves have been adjusted following Faltinsen [16] non-linear approximation for free decay tests:

$$\ddot{\xi} + p_1 \dot{\xi} + p_2 |\dot{\xi}| \dot{\xi} + p_3 \xi = 0, \tag{1}$$

where ξ is the motion (linear or angular), p_1 is linear damping coefficient, p_2 is quadratic damping coefficient and p_3 is the restoring coefficient. In order to evaluate wind influence on surge damping tests with and without wind have been performed. In Table 4 the coefficient values for selected repetitions are presented with WS (Wind Speed). It is remarkable the repeatability of the coefficients obtained from successive experiments. It is

interesting to observe that the natural period does not depend on wind speed. The quadratic term p_2 value is the largest contribution to damping, thus implying that viscous damping is the main dissipation mechanism. Linear damping associated with wave generation is small for frequencies close to the resonant ones.

In order to use these results in frequency domain linear codes, an equivalent linear damping p_{eq} is defined (see e.g. [17], where the third order damping term is assumed small):

$$p_{eq} = p_1 + \frac{8}{3\pi}\omega_1 X_1 p_2, \tag{2}$$

where ω_1 , this being a decay test, is the natural frequency and X_1 is a representative amplitude of the motion. Looking at the graphs in Fig. 4, it is evident that the damping is larger for large amplitudes while smaller for low angle oscillations later in the decay test. The equivalent linear damping accounts for this phenomenon by introducing a representative motion amplitude, which is dependent on the amplitudes of the motion under analysis (either survival or operational conditions). Later in the paper, motion amplitudes in surge of 8 meters in survival conditions will be documented. Being conservative, and considering the range of motions during the decay tests (see Fig.4) a more conservative value of 4 meters for X_1 in Eq. 2 to define the damping is sensible. With it, linear damping is of the order of 16% critical damping. The value is large compared to typical damping values of the order of 5% considered in literature for surge motion of offshore structures [17], although, strictly speaking, this value applies to soft-mooring conventional vessels. Actually, for a similar platform, Koo et al. [11] also reported surge damping values above 10% or even 20% [13] of critical one. While the motion is highly damped for large amplitude displacements, that is not the case for low amplitude motions and many cycles are required for the motion to be fully dampened out, as already reported by Jagdale&Ma [6] for a similar floater.

Regarding yaw motion, in Table 5 the damping results are presented. Also in this case, viscous damping is larger than linear damping. Equivalent linear damping considering typical yaw displacements of 1 degree in survival conditions is of the order of 8%. It is interesting that Koo et al. [13] report yaw damping values above 20% of critical.

RESULTS: REGULAR WAVE TEST (MOTION RAOS)

Regular wave tests have been performed in order to measure motion, tendon tension and acceleration RAOS. Results for two headings (0 and 45 deg) are briefly discussed next. The reasons for conducting 45 deg heading tests were:

1. To study response signals for seas with non-zero incident angle. This will be interesting to study the behavior but also

Test	T[s]	$p_1 [1/s]$	$p_2 [1/m]$
Surge WS 0m/s	25.19	0.0062	0.0927
Surge WS 0m/s	25.21	0.0069	0.0898
Surge WS 11.4m/s	25.25	0.0031	0.1090
Surge WS 11.4m/s	25.28	0.0053	0.1021

TABLE 4. Samples of surge decay tests.

Test	T[s]	$p_1 [1/s]$	p_2 [1/rad]
Yaw WS 0m/s	11.61	0.0315	7.2662
Yaw WS 0m/s	11.44	0.0173	8.2693

TABLE 5. Samples of yaw decay tests.

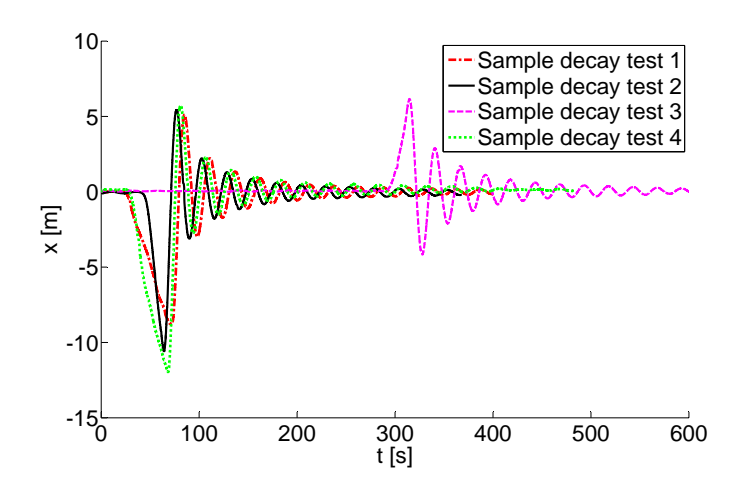


FIGURE 4. Repetitions of decay test in surge direction

to perform a more precise calibration for different heading seas to 0 deg.

2. To excite non fore-back motions (sway and roll) more significantly. In the 0 deg test, these sway and roll motions are very low. For the correlation analysis, it will be easier to have a more significant signal.

Heading 0 deg

The motion RAOs for this condition are presented in Fig. 8. Results are presented for surge, heave and pitch motions, which are the ones directly affected by waves with this heading. The responses in sway, roll and yaw are considered too small to be significant.

Maximum RAO in surge is 5 m/m, corresponding to natural period of TLPWT (25s) with the response amplification in operational seas ($T \sim 10s$) is lower than one. These values are similar

to Koo et al. [11, 13] in operational seas but larger than theirs for long wave periods. This difference, as mentioned when discussing decay tests, is partially due to the fact that Koo et al. installation depth is 200m compared to 80m in present design. As another example from literature, Naqvi [9] reports lower RAO values for surge than present research while responses for the other motions are similar.

A numerical estimation of surge RAO using IberdrolaFEM, an in-house developed software that couples potential flow/time domain hydrodynamic solver SEAFEM and the NREL aeroelastic FAST computational code, is presented in left panel of Fig. 8. The agreement with the experimental RAO can be considered good.

The response in pitch is below of 0.1 deg/m in periods of interest, but close to 4s is noticeable a resonant response corresponding to the natural period (see Table 3).

Maximum response in heave is around 0.18 m/m. It is relevant to mention that heave motion presents a response in double frequency due to its coupling with surge (set-down). This double frequency response in heave highlights the importance of heave natural period being as low as possible in order to avoid eventual resonant behavior in low period sea states. A time history of a sample regular test, where motion amplitudes have been divided by wave height, is presented in Fig. 5. The double frequency response in heave is evident from the time-series register. Due to the large stiffness of the tendons, the induced heave motion has as its maximum value the equilibrium position. In addition a significant surge response, consistent with the RAO presented in Fig. 8 is observed and low pitch motion can also be seen.

RAOs are estimated for different constant wind speeds (vin, vrated and vout), using the control algorithm presented below. It is worth mentioning that the wind effect turns out to be negligible in the regular waves motion RAOs.

Heading 45 deg

The results for this condition are displayed in Fig. 9. For symmetry reasons surge and Sway RAOs show a very similar trend, as expected. The response angular motion response has been negligible. The RAO in heave is similar to the one obtained for heading equal to 0deg.

RESULTS: IRREGULAR WAVE TEST Operational sea states

A range of operational conditions (OC) combining sea states, headings and wind speeds have been considered. Tests were conducted in UPM-CEHINAV model basin. One representative condition is discussed next. Theoretical wave spectrum (JONSWAP with peak enhancement factor of 3.3) for such representative test and the specific realization spectrum are presented in the top left panel of Fig. 10. The quality of the generated wave

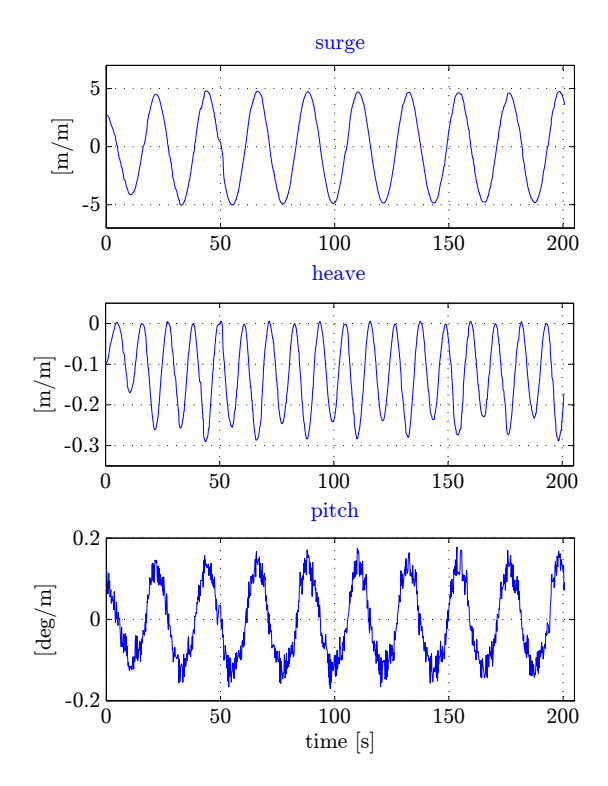


FIGURE 5. Sample time history of regular wave test $T_{wave} = 21.9s$.

is reasonable, with $T_p = 10.6s$, $H_s = 2.69$, compared to targeted $T_p = 10s$, $H_s = 2.5m$. The spectra of the tendon tensions are presented in the top right panel. Since the relevant quantity for the pontoon structural design is the net force due to the tendons tension, the sum of each pontoon tendons is analyzed. In these spectra, first order effects are clearly visible in the left part while higher frequency effects also appear at a frequency of 1.6 rad/s. These effects can be related to the fact that low amplitude pitch motion is excited at natural frequency. The importance of this phenomenon decreases rapidly for increasing wave period sea states.

Low frequency and low amplitude surge motion can be also observed in the surge spectra ($w \sim 0.25 rad/s$). This low frequency surge generates in turn the corresponding heave response and a small influence in low frequency tendon tension spectra. No high frequency (\sim 6 rad/s) resonant heave motion is found (high frequency parts of the curves not displayed because values are null).

The significant values of this case motions are presented in Table 6. The rms and maximum values of accelerations and tendon tensions are presented in Tables 7 and 8, respectively. After different discussions with common WT manufacturers, a very restrictive criteria has been imposed in terms of pitch angle and maximum acceleration (2 m/s^2 and 2 pitch degrees). The values are always lower than 0.54 degrees for pitch motion and al-

Test	surge	sway	heave	roll	pitch	yaw
	(m)	(m)	(m)	(deg)	(deg)	(deg)
OC	1.67	0.16	0.02	0.42	0.19	0.27
SC	8.99	1.57	0.81	0.22	1.39	0.73

TABLE 6. Motion significant values in wave irregular tests. Heading=0deg. WindDirection=0deg.

ways lower than $1.24 \, \text{m/s}^2$ for the maximum acceleration at nacelle, thus meeting the mentioned manufacturers criteria. This low operational values are common to the range of configurations tested. Limiting the pitch angle and nacelle accelerations ensures great stability and optimizes the downtime in comparison with other non-touted technologies.

Most loaded tendons are those situated upwind. Sway, roll and yaw motion effects on the small differences found on the maximum values measured in these two upfront cables.

Survival sea states

As previously mentioned, a range of 50 year return period survival conditions (SC) combining sea states, headings and a storm wind speed of 50m/s were considered. Tests were conducted in CEHIPAR ocean basin. One representative condition is discussed next. Theoretical wave spectrum (JONSWAP with peak enhancement factor of 3.3) for such representative test and the specific realization spectrum are presented in the top left panel of Fig. 11. The quality of the generated wave is reasonable with, $T_p = 14.3s$, $H_s = 14.5$ compared to targeted $T_p = 15.2s$, $H_s = 13.6m$. Tendon tensions spectra are presented in the top right panel. It can be observed that first order maximum response is significantly larger for downwind lines. This behavior occurs in all survival tests and no explanation for such phenomenon is yet available at this stage. Motion responses take place mainly in first order except heave motion where double frequency response is found, consistently with what was discussed when presenting regular waves motion RAOs. There are small low frequency responses in both heave and pitch motions that do not seem to generate any extra relevant response in tendon tensions. Again, the significant values of motions and rms and maximum values of accelerations and tendon tensions are displayed in Tables 6, 7 and 8, respectively. The maximum accelerations values in nacelle are below $3m/s^2$ and tensions are in all cases below 40% of MBL. Moreover, no slack event has been registered. These performance indicators are shared by the rest of tested survival conditions.

Acc.	xRms	xMax	yRms	yMax	zRms	zMax
	(m/s^2)	(m/s^2)	(m/s^2)	(m/s^2)	(m/s^2)	(m/s^2)
OC	0.14	0.53	0.02	0.06	0.02	0.09
SC	0.83	2.93	0.16	0.57	0.12	0.42

TABLE 7. RMS and MAX accelerations values in nacelle. Heading=0deg. WindDirection=0deg.

	L1 Max	L2 Max
	(kN)	(kN)
OC	2900.4	2786.0
SC	4070.3	4350.6

TABLE 8. MAX values most loaded (L1, L2) tendon tensions. Heading=0deg. WindDirection=0deg.

CONCLUSIONS

A comprehensive experimental campaign with a tension leg platform for an offshore wind turbine (TLPWT) has been carried out as request of IBERDROLA by CEHINAV-UPM model basin research group. The TLPWT tested has consisted of a central cylindrical column with four square section horizontal pontoons at its base, each pontoon moored with two tendons to the seabed. Operational, survival, failure and transport experiments have been conducted in different headings and with different wind conditions. The experimental setup, results from decay tests, regular wave motion RAOs, irregular wave responses, tendon loads and accelerations, have been presented and analyzed. Wind effect has been incorporated to the tests using a calibrated turbine, controlled with information obtained through real time platform motion tracking. The following conclusions have been obtained:

- The natural periods and damping values are similar to those reported in literature. Surge period has been found slightly lower than reference values, which is coherent with the fact that operation depth is in this case smaller than the common ones found in literature.
- 2. All motion RAOs are very small, except surge, consistently with the type of platform (TLP).
- 3. A maximum motion RAO of 5 in surge in a period range between 20-25s has been found. That value decays quadratically for lower periods leading to operational sea states RAOs that is lower than one.
- 4. Heave motion response in double frequency has been described, due to the coupling of surge and heave motions.
- 5. Operational conditions motions and accelerations RMS values fall within turbine manufactures operational limits, thus

- implying very low expected downtime in operational conditions.
- 6. Maximum accelerations values in nacelle are below $3m/s^2$ and tensions below 40% of MBL in survival conditions.
- 7. No slack occured.

Some future research lines follow naturally:

- 1. Wind loads have been introduced with a calibrated thrust miniature turbine. Certain uncertainties in regards to the blades induced damping remain.
- 2. The analysis of survival (failure) condition experiments conducted with a broken tendon.
- 3. The analysis of transportation experiments.
- 4. Second order effects have not been found significant in present campaign but further study is necessary.
- 5. VIV has been left out of the scope of present research but its importance is great for this type of structures.
- 6. Some issues in regards to upwind and downwind lines tension spectra in survival conditions have arisen, whose analysis is left for future research.

ACKNOWLEDGMENT

The authors are thankful to Elkin Botia-Vera, Hugo Ramos-Castro, Juan Luis Chacón, Amadeo Morán, Adriana Oliva, Patricia Alcanda, Luis Perez Rojas, Gabriele Bulian, Benjamin Bouscasse and Angel Martin (INSIA-UPM) for assisting in the experimental campaign and data processing.

REFERENCES

- [1] Henderson, A. R., Argyriadis, K., Nichols, J., and Langston, D., 2010. "Offshore wind turbines on TLPs assessment of floating support structures for offshore wind farms in german waters". In 10th German Wind Energy Conference.
- [2] Crozier, A., 2011. Design and dynamic modeling of the support structure for a 10 mw offshore wind turbine.
- [3] Bachynski, E. E., and Moan, T., 2012. "Design considerations for tension leg platform wind turbines". *Marine Structures*, **29**(1), pp. 89 114.
- [4] Bachynski, E. E., and Moan, T., 2013. "Hydrodynamic Modeling of Tension Leg Platform Wind Turbines". In ASME 32nd International Conference on Ocean, Offshore and Arctic Engineering, OMAE2013.
- [5] Bae, Y., and Kim, M., 2013. "Rotor-floater-tether coupled dynamics including second-order sum-frequency wave loads for a mono-column-TLP-type FOWT (floating off-shore wind turbine)". *Ocean Engineering*, 61(0), pp. 109 122.
- [6] Jagdale, S., and Ma, Q. W., 2010. "Practical simulation on motions of a TLP-type support structure for offshore wind

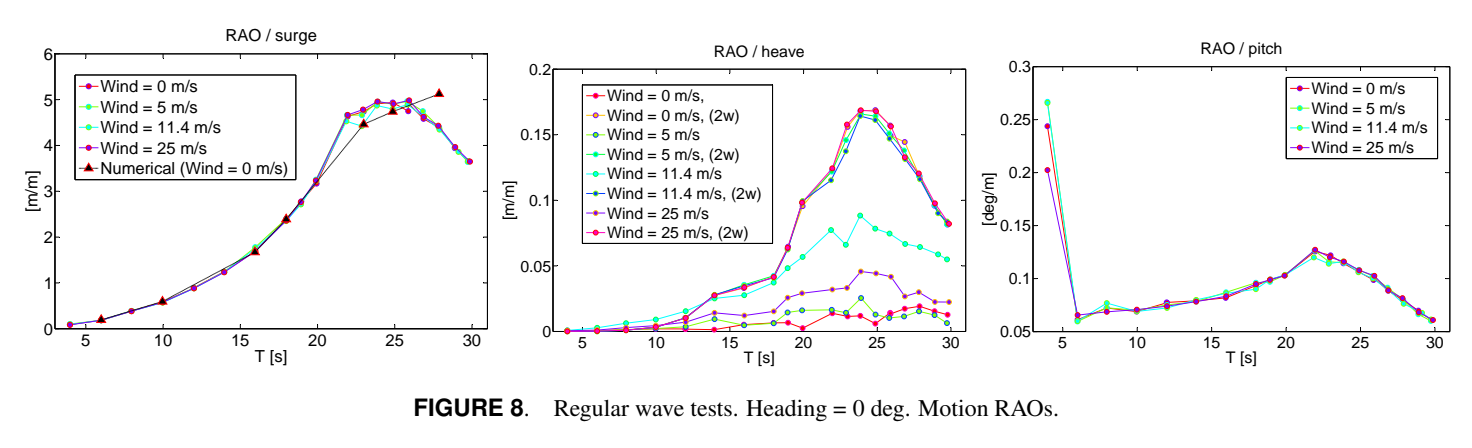
- turbines". In International Offshore and Polar Engineering Conference (ISOPE), The International Society of Offshore and Polar Engineers (ISOPE).
- [7] Nihei, Y., Kozen, M., and Iijima, K., 2012. "Elastic characteristics of TLP type offshore wind turbine". In ASME 31st International Conference on Ocean, Offshore and Arctic Engineering, OMAE2012.
- [8] Nihei, Y., Matsuura, M., Murai, M., Iijima, K., and Ikoma, T., 2013. "New design proposal for the TLP type offshore wind turbines". In ASME 32nd International Conference on Ocean, Offshore and Arctic Engineering, OMAE2013.
- [9] Naqvi, S. K., 2012. "Scale model experiments on floating offshore wind turbines". Master's thesis, Worcester Polytechnic Institute.
- [10] Thiagarajan, K. P., Urbina, R., and Hsu, W., 2013. "Non-linear pitch decay of a floating offshore wind turbine structure". In ASME 32nd International Conference on Ocean, Offshore and Arctic Engineering, OMAE2013.
- [11] Koo, B., Goupee, A. J., Lambrakos, K., and Lim, H. J., 2013. "Model test correlation study for a floating wind turbine on a tension leg platform". In ASME 32nd International Conference on Ocean, Offshore and Arctic Engineering, OMAE2013.
- [12] Goupee, A. J., Koo, B., Lambrakos, K., Kimball, R. W., and Dagher, H. J., 2012. "Experimental comparison of three floating wind turbine concepts". In ASME 31st International Conference on Ocean, Offshore and Arctic Engineering, OMAE2012.
- [13] Koo, B., Goupee, A. J., Lambrakos, K., and Kimball, R. W., 2012. "Model tests for a floating wind turbine on three different floaters". In ASME 31st International Conference on Ocean, Offshore and Arctic Engineering, OMAE2012.
- [14] Martin, H. R., Kimball, R. W., Viselli, A. M., and Goupee, 2012. "Methodology for wind/wave basin testing of floating offshore wind turbines". In ASME 31st International Conference on Ocean, Offshore and Arctic Engineering, OMAE2012.
- [15] DNV, June 2013. Design of Floating Wind Turbine Structures. Tech. Rep. DNV-OS-J103, Det Norske Veritas.
- [16] Faltinsen, O. M., 1990. Sea loads on ships and offshore structures / O.M. Faltinsen. Cambridge University Press.
- [17] Journee, J. M. J., and Massie, W. W., 2001. *Offshore Hydromechanics*. Delft University of Technology.



FIGURE 6. Transport and installation procedure simulation



FIGURE 7. TLPWT model in CEHINAV Model Basin (left) and in CEHIPAR Ocean Basin for survival tests (right).



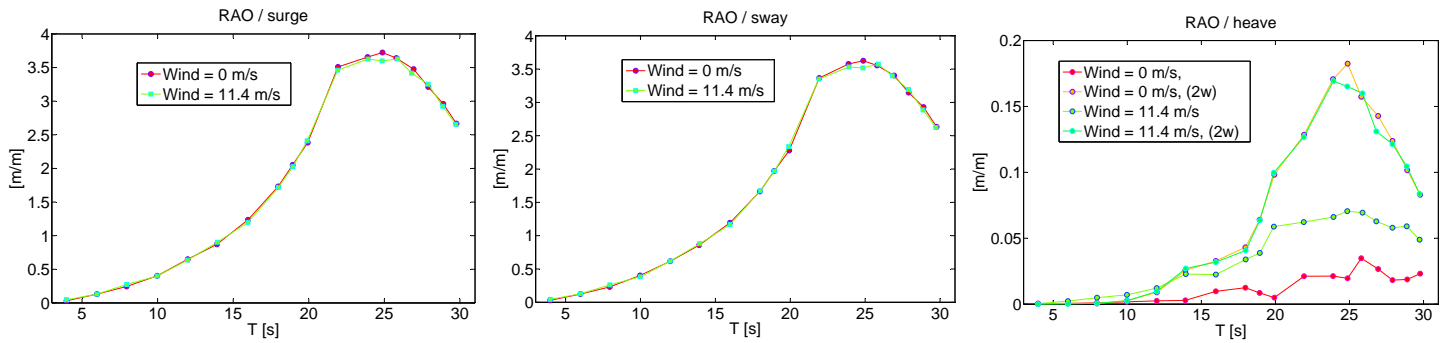


FIGURE 9. Regular wave tests. Heading = 45 deg. Motion RAOs.

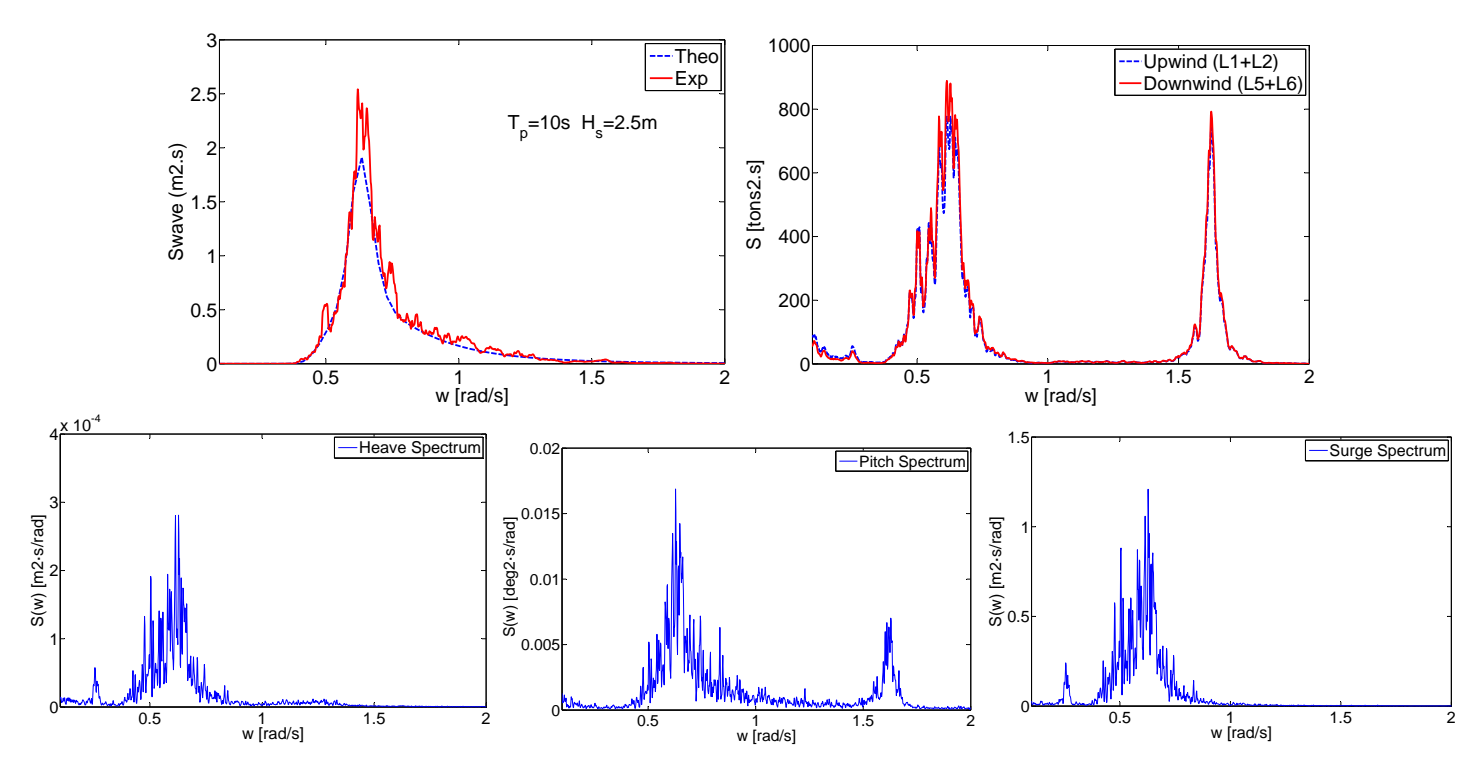


FIGURE 10. Sample operational irregular wave test results. Tp = 10s, Hs=2.5m, WindDirection=0deg, Heading=0deg, WindSpeed=11.4m/s. (Top left) wave spectrum. (Top right) tendon tension spectra. (Bottom from left to right) Heave, Pitch and Surge Spectra.

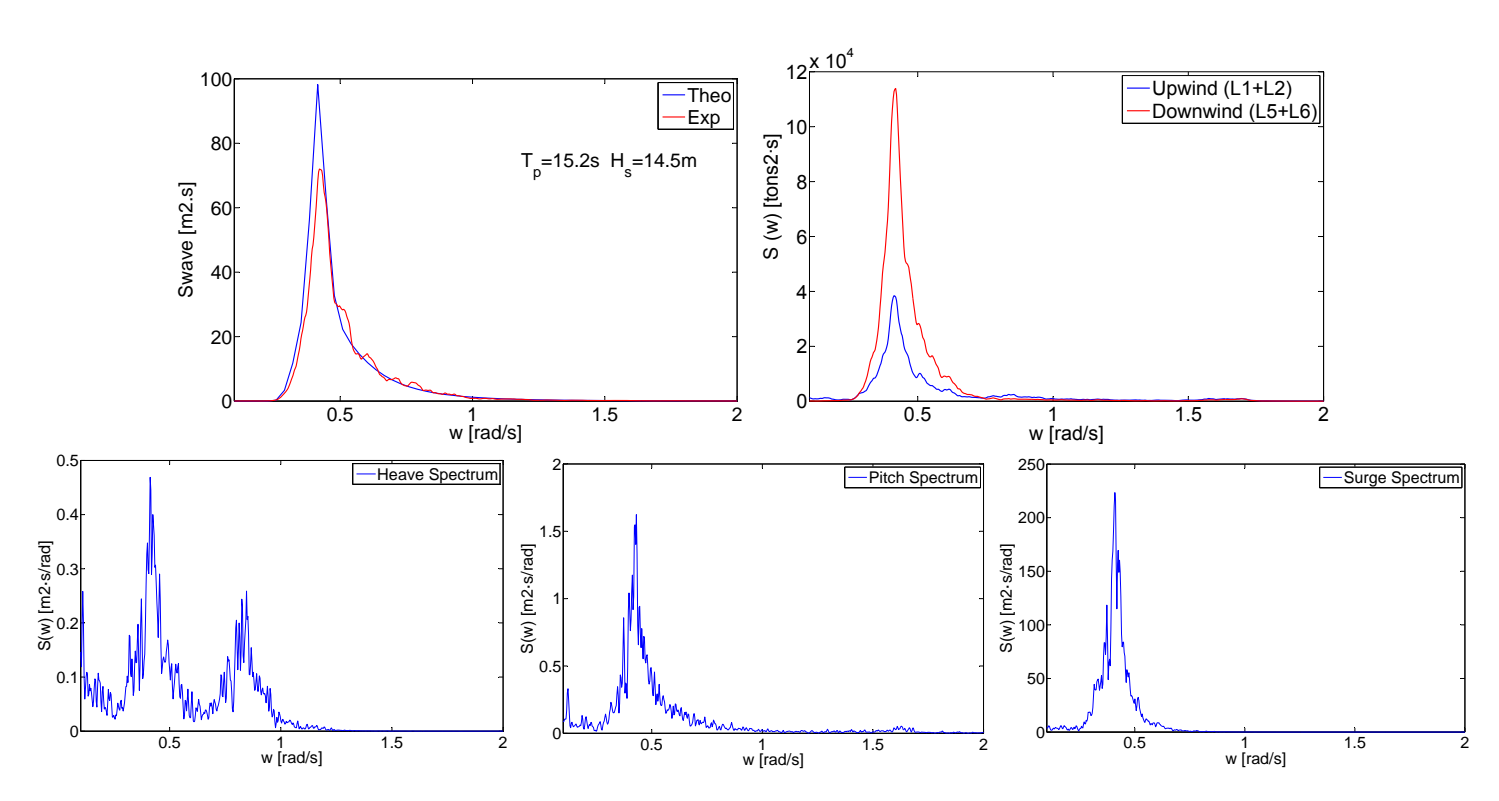


FIGURE 11. Sample survival irregular wave test results. Tp = 15.2s, Hs=14.5m, WindDirection=0deg, Heading=0deg, WindSpeed=50m/s. (Top left) wave spectrum. (Top right) tendon tension spectra. (Bottom from left to right) Heave, Pitch and Surge Spectra.